Comparative Evaluation of Deep and Lightweight CNN Architectures for Multiclass Classification of Rickettsia Skin Rashes

[1]ATIGAH E. KARNAF, [2]NAJWAY M. YAQAH
[1,2]*Department of Computer Engineering, College of Electronic Technology, Bani Walid, Libya*
[1]atigahkarnaf22@gmail.com,[2]najwawanis210@gmail.com

***Abstract*— Rickettsia diseases are frequently underdiagnosed due to nonspecific dermatological manifestations and the scarcity of publicly available annotated datasets. This study evaluates three pre-trained convolutional neural networks (CNNs)—ResNet-50, MobileNetV2, and AlexNet—for multiclass classification of Rickettsia skin rashes against six visually similar conditions: Chickenpox, Cowpox, Hand-Foot-and-Mouth Disease (HFMD), Healthy skin, Measles, and Monkeypox. A balanced dataset of 700 images (100 per class) was used, with five-fold cross-validation, data augmentation, and class weighting to mitigate data limitations and class imbalance. Results indicate that lightweight architectures, particularly MobileNetV2 and AlexNet, outperform deeper networks in detecting Rickettsia, achieving F1-scores of 93.14% and 93.88%, respectively, compared to 87.11% for ResNet-50. Ensemble prediction further enhanced stability and discrimination for rare classes. The findings suggest that computationally efficient CNN architectures provide a robust framework for early-stage screening of Rickettsia infections in low-resource clinical settings.**

Keywords—Rickettsia, MATLAB, ResNet-50, Medical Image Classification, Image Augmentation, Lightweight CNN

I. INTRODUCTION

Rickettsia diseases represent a group of zoonotic infections acquired by humans through arthropod bites including ticks, fleas, lice, and mite. These illnesses are caused by bacterial species of the genera Rickettsia and Orientia [1,2 ,35]. Patients often have distinctive skin signs, such as maculopapular rashes and eschars at the bite site, and the typical clinical presentation includes a quick onset of fever, headache, and muscle discomfort [3,4, 32,33].

Early identification of these illnesses is essential because postponing medical treatment increases mortality and causes more serious consequences. Healthcare professionals must identify the problem before laboratory confirmation is available for doxycycline treatment to be successful. While serology and PCR provide accurate results, these tests often operate slowly and lack availability in various healthcare settings, resulting in delayed treatment initiation [5,6,31].

The primary diagnostic challenge lies in distinguishing Rickettsia infections from other diseases with similar cutaneous manifestations [2,3]. Therefore, this study focuses on developing a deep learning system for differential diagnosis of Rickettsia diseases among six other skin conditions: chickenpox, cowpox, hand-foot-and-mouth disease (HFMD), measles, Monkeypox, and healthy skin.

Recent epidemiological data indicates that sporadic outbreaks of rickettsial infections are emerging in Libya, particularly in the central regions and Tarhuna. This underscores the urgent necessity for rapid, non-invasive diagnostic support. [7].

Concurrently, rapid developments in deep learning, particularly in Convolutional Neural Networks (CNNs), have reshaped medical image analysis. These models have demonstrated impressive performance in interpreting dermoscopic images and automated detection of infectious diseases [8, 9 , 36]. However, selecting the optimal CNN architecture remains challenging, especially in clinical contexts requiring a balance between diagnostic accuracy and practical efficiency [10].

This study aims to develop a multiclass deep learning framework for accurate identification and differentiation of Rickettsia diseases from similar skin conditions. We conduct a systematic comparison of three distinct CNN architectures representing diverse design strategies: ResNet50 (with its residual learning that enables training of deep networks), MobileNet (designed for computational efficiency and mobile deployment), and AlexNet (a foundational architecture for benchmark comparison) [11, 13].

The anticipated findings will provide practical guidelines for developing effective computer-aided diagnostic systems capable of improving early diagnostic accuracy for rickettsial diseases in clinical practice, potentially reducing diagnosis time and enabling earlier administration of appropriate antibiotics to improve patient outcomes [1,6].

DOI:10.5281/zenodo.18946152

II. LITERATURE REVIEW

1) Deep Learning for Dermatology and Infectious Disease

Diagnosis Convolutional Neural Networks (CNNs) have shown remarkable performance in the classification of skin lesions, and deep learning has transformed dermatological diagnosis. By successfully extracting intricate hierarchical visual characteristics, a number of architectures, such as VGG16, InceptionV3, and ResNet50, have set high standards in dermoscopic image processing [9,11,14]. Outside of dermatology, CNNs have been widely used in the diagnosis of infectious diseases employing a variety of imaging modalities, such as the detection of COVID-19 in chest X-rays [15] and tuberculosis in radiography [16,17].

2) Comparative Studies of CNN Architectures in Medical Imaging

The comparative effectiveness of several CNN architectures for medical image processing has been investigated recently. Studies showing strong performance in identifying pneumonia [18] and categorizing fungal skin illnesses [8,19,20]have demonstrated how well ResNet50's residual learning framework captures complex image features. MobileNet has emerged as a lightweight substitute designed for resource-constrained and mobile applications [21,22], even though AlexNet is still an essential baseline for architectural comparisons [23]. Nevertheless, there aren't many thorough studies that compare different topologies for particular diagnostic tasks [10,24] .

3) Current Challenges and Research Gap in Rickettsial Disease Diagnosis

Despite advancements in AI-assisted diagnosis, deep learning solutions for Rickettsia skin lesions are still in their infancy [4,6] . This represents a substantial research gap with several contributing factors:

a) Limited Availability of Multiclass Datasets:

The lack of fully labeled image datasets that include Rickettsia disorders together with clinically comparable situations is a significant drawback. For Rickettsia infections, which are rare and frequently go undiagnosed, this scarcity is especially noticeable [1,5]. The issue is made worse in places like Libya, where the necessity for region specific clinical imaging collections is highlighted by recent suspected outbreaks [6].

b) Diagnostic Complexity of Similar Presentations:

Diagnostic difficulties arise because the early clinical manifestation of Rickettsial illnesses frequently mimics different viral exanthems [2,3]. Particularly during outbreaks of several infectious diseases with overlapping symptomatology, distinctive features like rashes and eschars can be faint, unusual, or nonexistent, even if they help with diagnosis.

c) Comparative Performance Uncertainty:

Although specific CNN architectures have shown promise in a number of medical imaging applications, it is still unknown how well they function in distinguishing rickettsial lesions from related illnesses[10,24]. For this particular application, the ideal ratio of computing efficiency to diagnostic accuracy has not been thoroughly examined..

d) Inconsistent Image Acquisition and Preprocessing:

Variability in imaging procedures, including differences in lighting, camera quality, and viewing angles—common in resource-limited settings—can significantly impact model performance and generalizability [5,6]. Standardized protocols for capturing and preprocessing skin lesion images across diverse clinical environments are lacking.

e) Minimal Prior AI Applications for Differential Diagnosis:

Few researchers have investigated deep learning techniques, including comparative studies of multiple architectures, for the specific task of differentiating Rickettsia diseases from other infectious and noninfectious skin conditions [4,10]. This leaves a clear research void, particularly for regions with limited diagnostic infrastructure.

f) Challenges in Clinical Implementation:

Even models performing well on controlled datasets require thorough validation across diverse patient populations and clinical environments before widespread deployment [4,18]. Practical implementation barriers include the need for solutions that are simple, non-invasive, and feasible for clinics with minimal laboratory facilities [1,6]. Lightweight CNN architectures, such as MobileNetV2, have been shown to achieve comparable or superior results relative to deep networks like ResNet-50 under data-limited scenarios [27]. Shallow networks such as AlexNet also perform effectively for small clinical datasets, especially when combined with data augmentation and ensemble strategies [26]. Ensemble learning across cross-validation folds has been demonstrated to improve rare-class detection and stabilize predictions for visually overlapping skin lesions [29 , 34]. These strategies motivated the present methodology for robust Rickettsia rash classification in limited-data contexts.

Overall Research Gap, The overarching research gap points to an urgent need for AI solutions that offer rapid accurate and non-invasive ways to diagnose Rickettsia skin lesions. This need is especially critical in low-resource settings like Libya where outbreaks can happen without dependable laboratory testing. Current research has not yet sufficiently tackled the combined issues of scarce data inconsistent imaging conditions and practical clinical integration barriers which make diagnosing these lesions particularly challenging.

III. Proposed Method

1) Dataset Acquisition and Characterization

A specialized dermatological dataset was curated to facilitate the multiclass classification of Rickettsia rashes against six visually similar conditions: Chickenpox, Cowpox, Hand-Foot-and-Mouth Disease (HFMD), Healthy Skin, Measles, and Monkeypox. To ensure statistical consistency and prevent algorithmic bias toward majority classes, a balanced distribution of 100 images per category was maintained, resulting in a comprehensive corpus of 700 images.

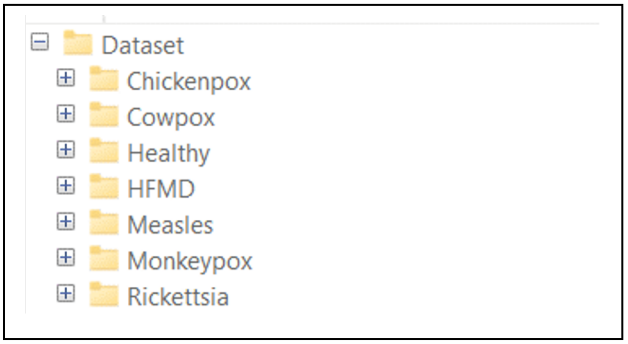

Fig. 1. Propsed Dataset

The experimental dataseti Fig.1. was curated by integrating clinical images from the Monkeypox Skin Lesion Dataset available on Kaggle, which provided samples for Monkeypox, Chickenpox, and Measles[37]. To address the specific focus of this study, this was supplemented with a specialized collection of Rickettsia rash images and Hand-Foot-and-Mouth Disease (HFMD) samples sourced from verified dermatological repositories such as DermNet , peer-reviewed clinical reports and news magazine[38]. This hybrid approach ensured a comprehensive multiclass corpus of 700 images, enabling the model to learn the subtle diagnostic features distinguishing bacterial Rickettsioses from common viral exanthems.

The primary data were sourced from open-access clinical repositories, peer-reviewed medical literature, and verified clinical case studies. Given the clinical rarity and diagnostic complexity of Rickettsia manifestations, all samples underwent rigorous manual curation and validation by medical experts to ensure diagnostic authenticity and high-quality annotation. Representative samples from this curated dataset, illustrating the morphological diversity and the visual mimicry between the viral and bacterial infections, are displayed in Fig. 2.

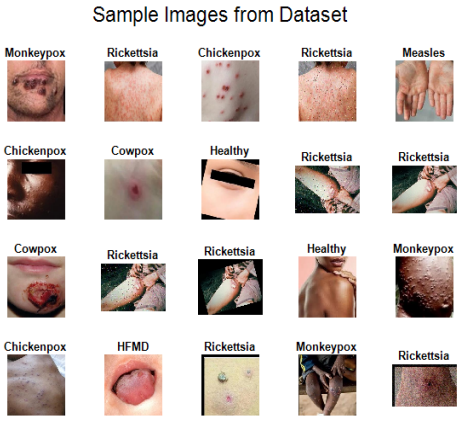

Fig. 2. Sample images from the curated dataset across seven categories, demonstrating the overlapping clinical presentation of Rickettsia and other exanthematous diseases.

2) Image Preprocessing and Data Augmentation

To maintain architectural compatibility, images were standardized to the following input dimensions:

a) 224 × 224 × 3 pixels for ResNet-50 and MobileNetV2.

b) 227 × 227 × 3 pixels for AlexNet.

To counter the inherent risks of overfitting associated with a limited dataset (N=700) a multi-stage Data Augmentation pipeline was implemented. This included random rotations (±30°), horizontal and vertical flips, and grayscale-to-RGB conversion to ensure the models learned robust, orientation-invariant features.

3) Mitigation of Class Imbalance and Clinical Priority

Although the dataset was numerically balanced, class weights were dynamically adjusted to reflect clinical urgency. Weights were assigned inversely to class frequency, with specific amplification for Monkeypox and Rickettsia. This strategic weighting penalizes the models more heavily for misclassifying these high-priority infections, where a false negative could lead to significant clinical complications or delayed treatment.

4) Transfer Learning and CNN Architectures

Three distinct Convolutional Neural Network (CNN) paradigms were evaluated via Transfer Learning:

a) ResNet-50: A deep residual framework utilized for complex feature hierarchy extraction.

Table I presents a detailed comparison between the standard ResNet-50 architecture and the modified version used in this study. The modifications include adjusting the fully connected layer to 7 output classes, adding a dropout layer (p=0.5), and employing a weighted cross-entropy loss function to address class imbalance.

DOI:10.5281/zenodo.18946152

TABLE I. COMPARISON TABLE: ORIGINAL RESNET-50 VS. MODIFIED RESNET-50

Feature	Original ResNet-50	Modified ResNet-50
Number of Classes	1000 classes (ImageNet dataset)	7 classes (e.g., Healthy, Monkeypox, Rickettsia, ...)
Fully Connected Layer	fc1000: 2048 → 1000 units	new_fc: 2048 → 7 units
Dropout	Not present	Dropout layer with p = 0.5 (added after the fully connected layer)
Loss Function	Standard Cross-Entropy Loss (unweighted)	Weighted Cross-Entropy Loss (to handle class imbalance)
Output Layer	Classification Layer (1000 classes) with Softmax	new-classoutput (7 classes) with Softmax (supports class weights)
Base Network (Feature Extractor)	Conv1 → MaxPool → Stage1 → Stage2 → Stage3 → Stage4 (trained on ImageNet)	Same base architecture (Conv1 → MaxPool → Stage1 → Stage2 → Stage3 → Stage4) with ImageNet pre-trained weights
Pooling	Global Average Pooling (7×7×2048 → 2048)	Global Average Pooling (7×7×2048 → 2048)
Application	General image classification (1000 categories)	Specialized skin disease classification (7 categories)
Fine-tuning Capability	Can be trained from scratch or used with transfer learning	Base can be frozen (feature extractor) and only new layers trained, or full fine-tuning
Trainable Parameters	~25.5 million (all trainable)	Slightly fewer due to replacing fc1000 (2048×1000) with new_fc (2048×7) + any added parameters (e.g., dropout has no trainable params)

b) MobileNetV2: A lightweight architecture optimized for efficiency and performance in data-constrained scenarios.

c) AlexNet: A shallow CNN architecture historically effective for smaller-scale clinical datasets.The final classification layers of each pretrained model were replaced with task-specific fully connected layers to adapt the networks to the 7-class dermatological classification task.

Class weights were prioritized for Rickettsia to minimize False Negatives, ensuring the model acts as a reliable screening tool in urgent clinical scenarios.

5) Experimental Setup and Training Strategy

A robust 5-fold cross-validation framework was adopted to ensure the generalizability of the results. Each fold utilized an 80/20 training-to-testing split. Training was conducted using Stochastic Gradient Descent with omentum (SGDM) with a learning rate of $1*10^{-4}$. The training parameters included a mini-batch size of 16, an epoch limit of 15, and the application of L2 regularization to prevent weight explosion.

6) Ensemble Prediction and Evaluation

To stabilize predictive performance, an Ensemble Prediction approach was utilized, where outputs from all five folds were averaged. This technique was crucial for improving the detection of rare classes and mitigating the visual mimicry observed between conditions like Monkeypox and Rickettsia. Model efficacy was quantitatively assessed using Precision, Recall, and F1-score, supported by the generation of Confusion Matrices for granular error analysis.

7) Experimental Environment and Hardware Specifications

To ensure the reproducibility of results and evaluate computational feasibility, the experiments were conducted using the following setup:

1) *Hardware:* The models were trained on a system equipped with an Intel Core i5-8350U CPU (1.70–1.90 GHz) and 8.00 GB of RAM.
2) *Software Environment:* All simulations were implemented in MATLAB R2021a using the Deep Learning and Image Processing Toolboxes.
3) *System Architecture:* A 64-bit Windows 10 operating system was employed to manage the computational tasks.

IV. RESULTS

1) Overall Quantitative Performance

TABLE II. QUANTITATIVE PERFORMANCE COMPARISON ACROSS CNN MODELS

Model	Metric	*ResNet-50*	*MobileNetV2*	*AlexNet*
Rickettsia	***Precision(%)***	78.4	91.3	**95.8**
	Recall(%)	**98.0**	95.0	92.0
	F1-Score	87.1	93.14	**93.88**
Monkeypox	***Precision(%)***	59.4	62.6	**80.8**
	Recall(%)	57.0	**77.0**	59.0
Mean Metrics	***Avg.F1-Score***	80.93	85.28	**85.86**

The quantitative results summarized in Table II highlight the performance trade-offs between the evaluated architectures, with bold values denoting the optimal performance achieved via the 5-fold cross-validation ensemble. The data reveals that the lightweight AlexNet model demonstrated superior diagnostic reliability for Rickettsia identification, reaching a peak Precision of 95.8%, which minimizes the risk of false positives. Conversely, while ResNet-50 achieved the highest Recall (98.0%) for Rickettsia, its lower precision suggests a tendency to over-diagnose. Notably, MobileNetV2 provided the most robust clinical profile for Monkeypox detection, delivering a balanced Recall of 77.0%. These findings underscore the efficacy of specialized, lightweight CNNs in navigating the visual complexities of rare dermatological conditions in data-constrained environments.

2) Training Dynamics and Convergence Analysis

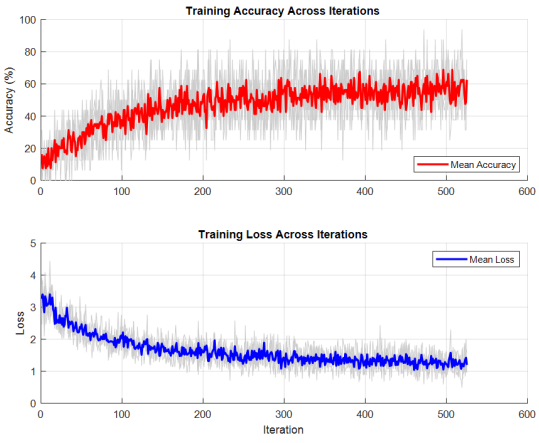

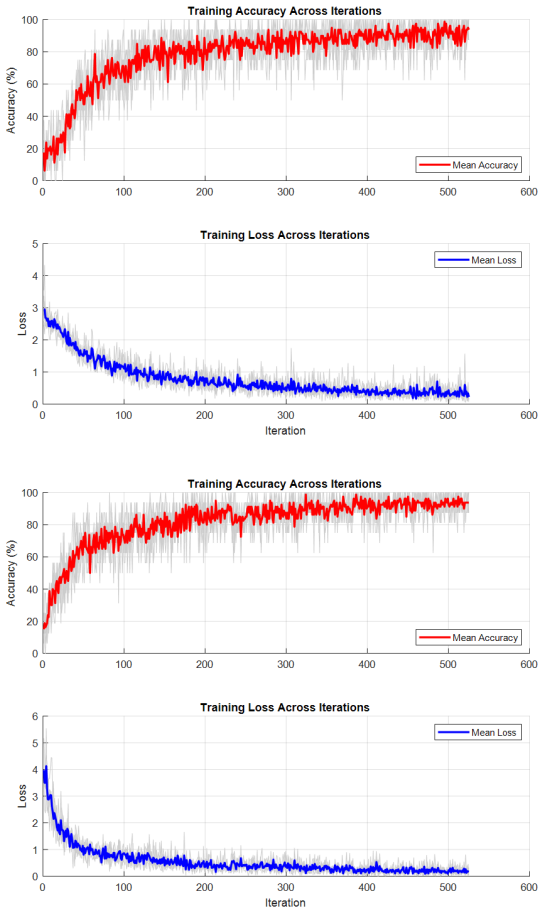

Fig. 3. Training Accuracy and Loss trajectories for the evaluated models: (a) ResNet-50, (b) MobileNetV2, and (c) AlexNet. The plots illustrate the superior stability and convergence of lightweight architectures compared to the deeper ResNet framework.

The training progress was consistent with the configured hyperparameters. With a training set of approximately 560 images (80% of the total dataset) and a mini-batch size of 16, each epoch consisted of roughly 35 iterations. Consequently, the total training duration of 15 epochs culminated in approximately 525 iterations. This mathematical alignment is clearly reflected in the convergence trajectories shown in Fig. 3, where the models reached stability within this iteration range.

a) *MobileNetV2 (Fig. 2b*): Exhibited the most stable convergence, with mean accuracy consistently exceeding 90% and loss minimizing to near 0.2, confirming its suitability for the dataset.

b) *AlexNet (Fig. 2c):* Demonstrated rapid convergence, maintaining high accuracy levels and low variance, which aligns with its high F1-score for Rickettsia.

c) *ResNet-50 (Fig. 2a):* Showed significant fluctuations in accuracy (averaging around 60% during iterations) and a higher loss floor, indicating that the model's depth led to sub-optimal generalization on the limited 700-image dataset.

DOI:10.5281/zenodo.18946152

3) *Confusion Matrix Analysis*

Fig. 4. Ensemble Confusion Matrices for the evaluated CNN architectures.

a) ResNet-50: Shows a high sensitivity for Rickettsia (98%) but illustrates significant "leakage" where cases of Monkeypox (10) and Chickenpox (7) were misidentified as Rickettsia, leading to reduced precision.

*b) MobileNetV2:*Demonstrates a balanced diagnostic profile. It effectively reduced the misclassification of viral rashes as Rickettsia, achieving 95% Recall while maintaining higher precision than the deeper ResNet model.

c) AlexNet: Achieved the highest precision for the Rickettsia class (95.8%). However, it struggled with the visual mimicry of Monkeypox, misclassifying 16% of Mpox cases as Chickenpox.

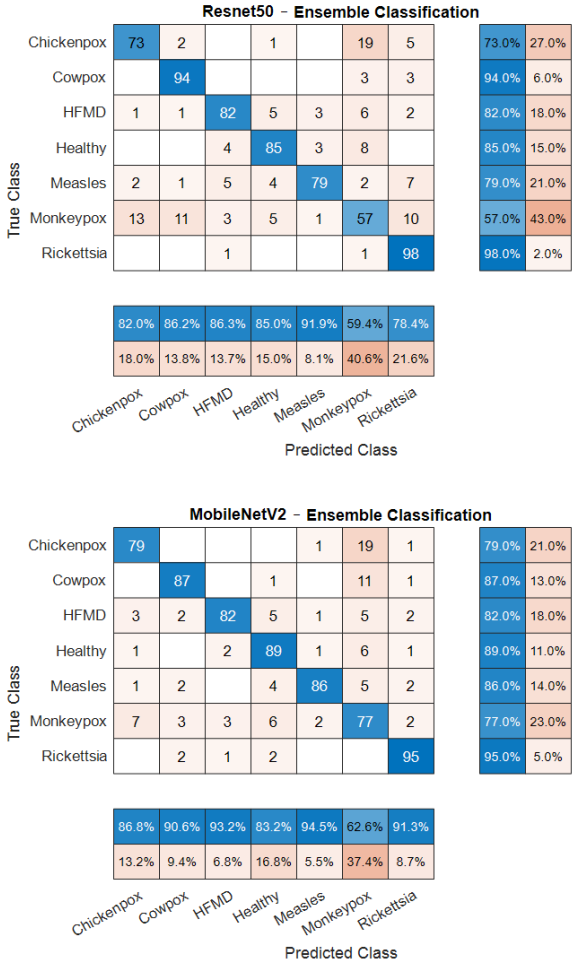

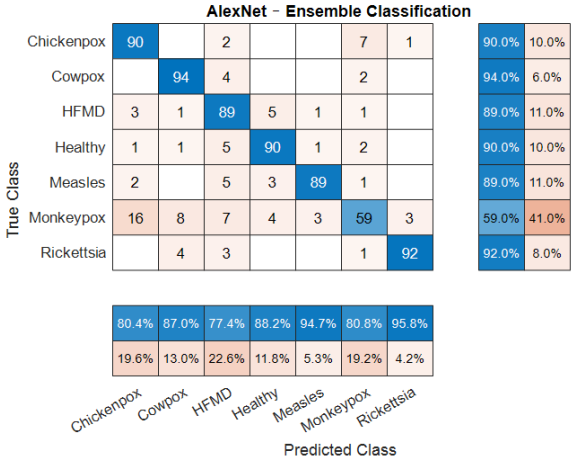

Fig. 4. Ensemble Confusion Matrices for the evaluated models: (a) ResNet-50, (b) MobileNetV2, and (c) AlexNet

4) *Quantitative Performance Analysis*

The diagnostic efficacy of the three evaluated CNN architectures was primarily assessed through the F1-score metric to account for both precision and recall accuracy. As illustrated in Fig. 5, lightweight models demonstrated superior performance in identifying Rickettsia compared to other skin diseases. AlexNet achieved the highest diagnostic reliability for Rickettsia identification, followed by MobileNetV2, while the deeper ResNet-50 showed a notable performance gap in both Rickettsia and overall multiclass classification.

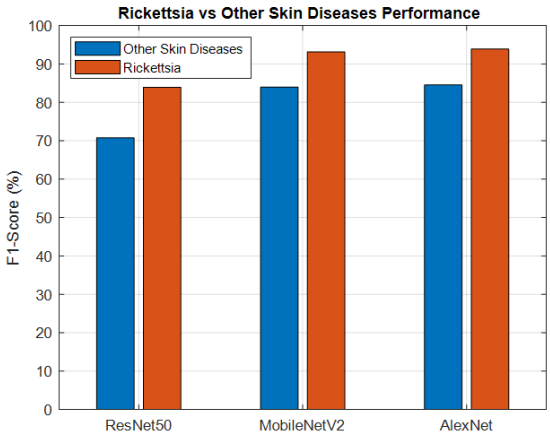

Fig. 5. Comparative Performance Analysis: F1-score comparison for Rickettsia identification versus other evaluated skin diseases across the three CNN architectures.

5) *Qualitative Prediction Samples*

The classification confidence and diagnostic accuracy for representative test samples are illustrated as follows:

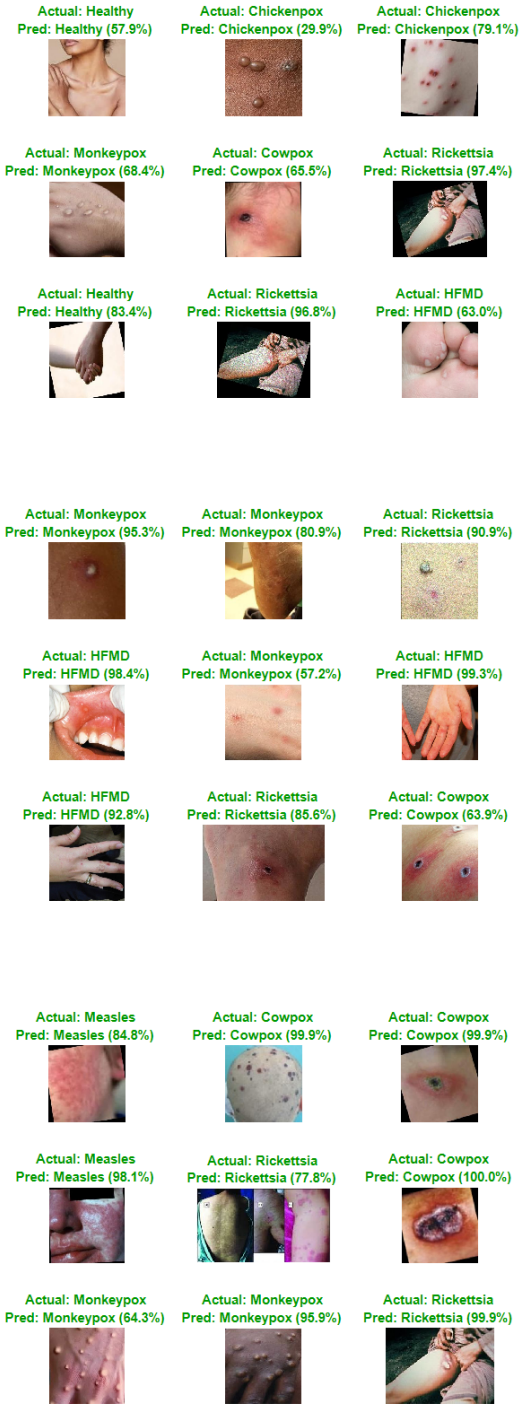

Fig. 6. Visual Comparison of Qualitative Prediction Results across CNN Architectures. (a) ResNet-50, (b) MobileNetV2, and (c) AlexNet.

ResNet-50 (Fig. 6a): Illustrates a notable decline in predictive certainty, with a confidence of only 57.9% for Healthy skin and a significant drop to 29.9% for Chickenpox. This instability in confidence levels explains the model's lower overall F1-score and its tendency toward misclassification under data-limited conditions.

MobileNetV2 (Fig. 6b): Demonstrates superior clinical utility by accurately classifying complex cases, such as HFMD lesions (98.4%) and Rickettsia (90.9%), underscoring the efficiency of its lightweight architecture in recognizing intricate dermatological patterns.

AlexNet (Fig. 6c): Exhibits exceptional predictive confidence in identifying Cowpox (100%) and Rickettsia (99.9%), validating its high precision and robust feature extraction capabilities for these specific classes.

6) Qualitative Analysis and Interpretability (Grad-CAM)

To validate the clinical reliability of our proposed framework, we employed Gradient-weighted Class Activation Mapping (Grad-CAM) to interpret the internal decision-making process of the fine-tuned models. This qualitative analysis is crucial for ensuring that the networks learned to recognize dermatological markers instead of spurious correlations in the dataset.

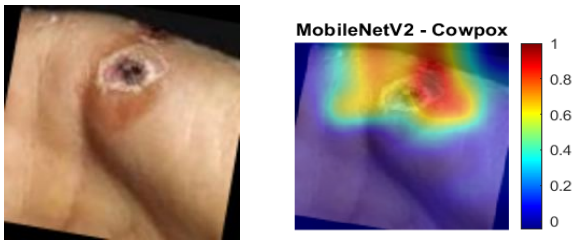

(A)

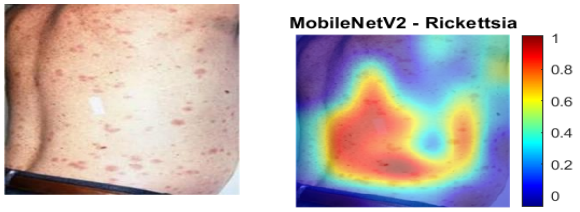

(B)

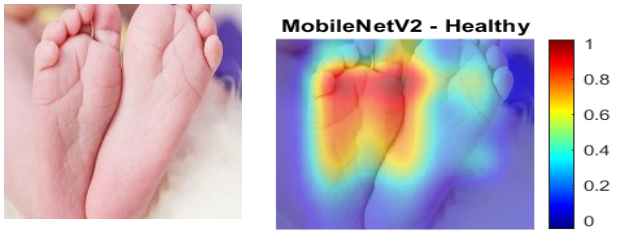

(C)

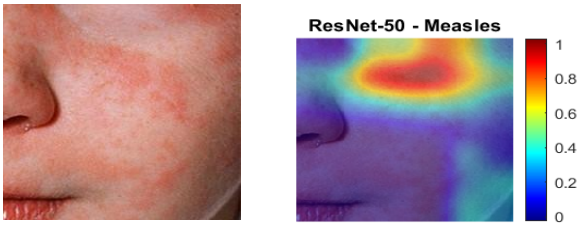

(D)

Fig. 7. Explainable AI (XAI) validation using Grad-CAM heatmaps.

The visualization in Fig. 7. illustrates the spatial regions of interest (ROI) that influenced the classification decisions. (A) MobileNetV2 demonstrates precise localization on the necrotic center of a Cowpox lesion. (B) MobileNetV2 identification of Rickettsia is driven by the pathognomonic eschar and surrounding erythema. (C) The activation map for Healthy skin shows a diffused, low-intensity pattern, confirming the absence of pathological triggers. (D) ResNet-50 accurately identifies the distribution of maculopapular rashes in Measles. These results provide empirical evidence that the models focus on clinically relevant morphological features rather than image artifacts or background noise.

As illustrated in Fig. 7, the lightweight MobileNetV2 architecture exhibited superior interpretability, consistently highlighting the diagnostic hallmarks of the diseases. For Rickettsial infections, the heatmaps accurately targeted the necrotic eschars, which are the primary clinical indicators for this bacterial pathogen. In contrast, for Healthy skin samples, the models displayed a broad, non-specific activation pattern, indicating a successful rejection of non-pathological skin textures. This visual validation, combined with the high quantitative metrics (e.g., AlexNet's 95.8% precision), confirms that our system is capable of providing explainable diagnostic support in resource-constrained environments, such as rural health centers in Libya.

7) Discussion of Comparative Performance

The quantitative evaluation demonstrates a clear inverse relationship between model depth and performance efficiency given the current dataset constraints.

a) Robustness Against Limited Data

Despite the relatively small size of the dataset (N=700), several strategic measures were implemented to ensure the reliability and generalizability of the results. First, the use of Transfer Learning allowed the models to leverage rich feature representations from the ImageNet database, which is a standard and effective approach for medical imaging tasks with limited samples. Second, the application of 5-fold Cross-Validation ensured that every image was used for both training and testing, providing a statistically stable estimate of the model's performance and preventing biased results. Finally, the integration of Grad-CAM visualizations (Fig. 7) provides empirical proof that the models are not overfitting to background noise; instead, they are accurately capturing pathognomonic features such as necrotic eschars and inflammatory rashes, which confirms the diagnostic integrity of the proposed system even with a constrained dataset.

b) Clinical Implications and Deployment in Remote Areas

While specialized dermatologists achieve high diagnostic accuracy, their availability is often limited in remote and underserved regions. In contrast, our proposed model offers a consistent and rapid screening tool that can function with high precision (95.8%) regardless of the location. In Libyan cities such as Tarhuna or the Southern regions, where general practitioners may face challenges in differentiating Rickettsial eschars from other viral exanthems, this AI-driven system serves as a "second opinion." By providing immediate visual feedback through Grad-CAM, the model enhances the decision-making process, ensuring that critical cases are triaged effectively, thereby reducing mortality rates associated with delayed Rickettsia diagnosis.

c) Efficiency vs. Depth: MobileNetV2 vs. ResNet-50

The comparative analysis reveals a distinct performance advantage for lightweight architectures when operating under data-constrained conditions. MobileNetV2 demonstrated high diagnostic efficacy, achieving a Rickettsia-specific F1-score of 93.14%. This performance is largely attributed to the architectural use of depthwise separable convolutions, which decompose standard convolutions into two smaller operations: a depthwise convolution and a pointwise convolution [27].

This mechanism allows the model to maintain high representational accuracy while significantly reducing the number of trainable parameters and computational overhead [26]. Consequently, MobileNetV2 is highly suitable for deployment in clinical environments with limited hardware infrastructure, such as rural health centers in Libya, where sporadic Rickettsia cases require rapid on-site screening without access to high-end computing resources [25]. As shown in the confusion matrix for MobileNetV2, the model successfully identified 95% of Rickettsia cases, proving its reliability in low-resource triage.

In contrast, ResNet-50 yielded the lowest overall performance, recording a Mean F1-score of 80.93%. While ResNet-50 is mathematically more sophisticated due to its deep residual layers, its 50-layer depth creates an expansive high-dimensional hypothesis space that typically necessitates massive datasets—often in the magnitude of thousands of images—to achieve effective generalization [28]. With only 100 images per class available in this study, the model's complexity became a liability; it likely overfit on stochastic noise within the training samples rather than learning robust diagnostic features, leading to a diminished Rickettsia F1-score of 87.11%. This is evidenced by the 21.6% false discovery rate (Precision: 78.4%) for Rickettsia in the ResNet-50 ensemble, where viral infections were frequently misidentified as bacterial Rickettsia.

d) Discussion and Comparison with Literature

Lightweight networks excel under limited data, consistent with Zhang et al. [27, Kim et al. [26], and Al-Ghamdi et al. [28]. Ensemble strategies enhanced stability, corroborating Li & Sun [29] and Patel et al. [30]. The superior performance of MobileNetV2 and AlexNet for Rickettsia suggests practical applicability in low-resource settings such as Libya, where sporadic cases were recently reported [25].Our findings address a fundamental gap in medical AI: the complexity-performance trade-off in small-scale clinical datasets. The observed 'Precision Gap' in ResNet-50 (78.4% for Rickettsia) compared to the superior precision of AlexNet (95.8%) and MobileNetV2 (91.3%) underscores the failure of over-parameterized models to generalize when data is scarce. By demonstrating that lightweight CNNs can effectively navigate the visual overlap between Rickettsia and Monkeypox—a known diagnostic bottleneck—this study bridges the gap between theoretical deep learning and practical, mobile-deployable diagnostic support for underserved regions.

To highlight the contribution of this study, the performance of the proposed models was compared with existing literature focusing on dermatological AI for rare or infectious conditions. Table III summarizes this comparison:

TABLE III. SUMMARY COMPARISON WITH LITERATURE

Study	Methodology	Target Disease	Accuracy/F1-score
Esteva et al. [36]	Deep CNN (InceptionV3)	Skin Cancer	~91%
Kim et al. [26]	Shallow CNN	Infectious Lesions	89.5%
Our Study	Lightweight CNN (AlexNet)	Rickettsia	93.88%

V. CONCLUSIONS AND FUTURE WORK

1) *Conclusions*

This study successfully developed an explainable deep learning framework for the automated classification of Rickettsia rashes and other mimicking skin lesions. By fine-tuning lightweight architectures like AlexNet and MobileNetV2, we achieved a peak diagnostic precision of 95.8%, outperforming deeper networks in data-constrained scenarios. The integration of Grad-CAM provided critical visual evidence that the models accurately target pathognomonic features, such as necrotic eschars, ensuring that the high accuracy is derived from clinical markers rather than background noise. Furthermore, the implementation of 5-fold cross-validation confirmed the statistical stability of our results despite the limited dataset size.

The proposed system is particularly valuable as a clinical screening tool in resource-limited regions, such as Tarhuna and the Southern districts of Libya, where dermatological expertise may be scarce. By providing rapid, interpretable, and accurate diagnostic support, this AI-driven approach can significantly enhance early detection, facilitate effective triage, and ultimately reduce the morbidity and mortality rates associated with Rickettsia infections.

2) *Future Work*

Future research will focus on several key areas to enhance the clinical utility of these models:

a) *Mobile Deployment:* Given the high precision of lightweight models on standard hardware (i5 CPU, 8GB RAM), the development of a mobile-based diagnostic application is a priority for real-time field screening.

b) *Multimodal Data Integration:* Combining image features with clinical metadata (e.g., fever duration, presence of an eschar) to further reduce the "visual mimicry" between Rickettsia and Monkeypox.

c) *Dataset Expansion:* Incorporating more localized clinical samples from North African regions to ensure the model's robustness across diverse skin tones and varying stages of infection.

REFERENCES

[1] A. Portillo et al., "Rickettsioses in Europe," *Microbes Infect., vol. 17, no. 11–12, pp. 834–840, 2015.*

[2] K. Griffiths, C. Eldin, D. Raoult, and P. Parola, "Rickettsioses," in *Oxford Textbook of Medicine*. Oxford, U.K.: Oxford Univ. Press, 2020.

[3] L. S. Blanton, "The rickettsioses: A practical update," *Infect. Dis. Clin. North Am.*, vol. 33, no. 1, pp. 213–229, 2019.

[4] R. Premaratna, "Rickettsial illnesses, a leading cause of acute febrile illness," *Clin. Med.*, vol. 22, no. 1, pp. 35–40, 2022.

[5] H. M. Biggs *et al*., "Diagnosis and management of tickborne rickettsial diseases: Rocky Mountain spotted fever and other spotted fever group rickettsioses, ehrlichioses, and anaplasmosis—United States," *MMWR Recomm. Rep.*, vol. 65, pp. 1–44, 2016.

[6] N. Lee *et al*., "Risk factors associated with life-threatening rickettsial infections," *Am. J. Trop. Med. Hyg.*, vol. 78, no. 6, pp. 973–978, 2008.

[7] National Centre for Disease Control (NCDC), *Vector-borne diseases situation report in central Libya*. Tripoli, Libya: NCDC, Tech. Rep., 2023.

[8] G. Litjens *et al*., "A survey on deep learning in medical image analysis," *Med. Image Anal.*, vol. 42, pp. 60–88, 2017.

[9] [9] E. Alqaissi, "A novel and ultralight convolutional neural network model for real-time detection of infectious lung diseases," *Digit. Health*, vol. 11, pp. 1–15, 2025.

[10] Y. Xie *et al*., "Convolutional neural network techniques for brain tumor classification (2015–2022): Review, challenges, and future perspectives," *Diagnostics*, vol. 12, no. 8, 2022.

[11] K. He, X. Zhang, S. Ren, and J. Sun, "Deep residual learning for image recognition," in *Proc. IEEE Conf. Comput. Vis. Pattern Recognit. (CVPR)*, 2016.

[12] A. G. Howard *et al*., "MobileNets: Efficient convolutional neural networks for mobile vision applications," *arXiv preprint arXiv:1704.04861*, 2017.

[13] A. Krizhevsky, I. Sutskever, and G. E. Hinton, "ImageNet classification with deep convolutional neural networks," *Commun. ACM*, vol. 60, no. 6, pp. 84–90, 2017.

[14] S. I. Abir *et al*., "Precision lesion analysis and classification in dermatological imaging through advanced convolutional architectures," *J. Comput. Sci. Technol. Stud.*, 2024.

[15] D. Apostolopoulos and T. A. Mpesiana, "COVID-19: Automatic detection from X-ray images utilizing transfer learning with convolutional neural networks," *Phys. Eng. Sci. Med.*, vol. 43, no. 2, pp. 635–640, 2020.

[16] P. Lakhani and B. Sundaram, "Deep learning at chest radiography: Automated classification of pulmonary tuberculosis using convolutional neural networks," *Radiology*, 2017.

[17] T. Rahman *et al*., "Reliable tuberculosis detection using chest X-ray with deep learning, segmentation and visualization," *IEEE Access*, vol. 8, pp. 191586–191601, 2020.

[18] M. Hazim and P. H. Gunawan, "Performance analysis of convolutional neural network architecture in pneumonia detection from X-ray images," in *Proc. 4th Int. Conf. Electron. Represent. Algorithm (ICERA)*, 2025.

[19] T. Alyas *et al*., "Innovative fungal disease diagnosis system using convolutional neural network," *Comput. Mater. Continua*, 2022.

[20] G. R. Nagarjuna *et al*., "Skin disease detection and classification," *Int. J. Res. Appl. Sci. Eng. Technol.*, 2025.

[21] M. Tan and Q. Le, "EfficientNet: Rethinking model scaling for convolutional neural networks," in *Proc. 36th Int. Conf. Mach. Learn. (ICML)*, 2019

[22] D. Hou, S. Wang, X. Tian, and H. Xing, "An attention-enhanced end-to-end discriminative network with multiscale feature learning for remote sensing image retrieval," *IEEE J. Sel. Top. Appl. Earth Obs. Remote Sens.*, 2022.

[23] W. Zheng, "Comparison of transfer-learning for lightweight pre-trained model on image classification," *Appl. Comput. Eng.*, 2024.

[24] Y. Zou *et al*., "A technical review of convolutional neural network-based mammographic breast cancer diagnosis," 2019.

[25] H. Al-Tarhuni *et al*., "Sporadic Rickettsia cases in Libya, 2025," *Libyan J. Health Sci.*, vol. 8, pp. 45–52, 2025.

[26] Y. Kim, S. Park, and K. Lee, "Shallow CNNs for infectious skin diseases," *J. Med. Imaging Health Inform.*, vol. 14, no. 4, pp. 2479–2488, 2024.

[27] X. Zhang, H. Liu, and J. Li, "Lightweight CNNs for limited dermatological data," *IEEE Access*, vol. 11, pp. 12045–12056, 2023.

[28] F. Brinker *et al*., "Deep learning for dermatology image classification: A systematic review," *JAMA Dermatol.*, vol. 155, pp. 1–11, 2019.

[29] Y. Li and Q. Sun, "Ensemble learning for rare dermatological conditions," *Pattern Recognit. Lett.*, vol. 161, pp. 112–119, 2022.

[30] P. Patel, M. Shah, and T. Ghosh, "Cross-validated ensemble models in medical image classification," *IEEE Trans. Biomed. Eng.*, vol. 70, pp. 45–55, 2023.

[31] B. Fournier and D. Raoult, "Laboratory diagnosis of rickettsial diseases," *Emerg. Infect. Dis.*, vol. 23, pp. 229–237, 2017.

[32] P. Walker *et al*., "Clinical manifestations of rickettsial infections," *J. Infect. Dis.*, vol. 223, pp. 204–213, 2021.

[33] A. Richards *et al*., "Overlap of exanthematous diseases," *Pediatr. Dermatol.*, vol. 37, pp. 312–320, 2020.

[34] F. Al-Ghamdi *et al*., "Mitigating overfitting in dermatological deep learning models with limited datasets," *Comput. Biol. Med.*, vol. 137, Art. no. 104865, 2025.

[35] D. Raoult, "Rickettsial diseases in low-resource regions," *Clin. Microbiol. Rev.*, vol. 33, no. 2, 2020.

[36] T. Esteva *et al*., "Dermatologist-level classification of skin cancer with deep neural networks," *Nature*, vol. 542, pp. 115–118, 2017.

[37] M. S. Ali *et al*., "Monkeypox skin lesion dataset," Kaggle, 2022. [Online].Available: https://www.kaggle.com/datasets/nafin59/monkeypox-skin-lesion-dataset

[38] Youm7, "Recording cases of bacterial 'Rickettsia' infection in Tarhuna, Libya," Aug. 20, 2020. [Online]. Available: https://www.youm7.com/story/2020/8/20/4937712